
This is an electronic reprint of the original article.
This reprint may differ from the original in pagination and typographic detail.

Le, Nguyen-Duc; Trogen, Mikaela; Ma, Yibo; Varley, Russell J.; Hummel, Michael; Byrne, Nolene

Cellulose-lignin composite fibres as precursors for carbon fibres. Part 2 - The impact of precursor properties on carbon fibres

Published in:
Carbohydrate Polymers

DOI:
[10.1016/j.carbpol.2020.116918](https://doi.org/10.1016/j.carbpol.2020.116918)

Published: 15/12/2020

Document Version
Peer-reviewed accepted author manuscript, also known as Final accepted manuscript or Post-print

Published under the following license:
CC BY-NC-ND

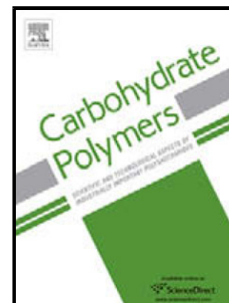
Please cite the original version:
Le, N.-D., Trogen, M., Ma, Y., Varley, R. J., Hummel, M., & Byrne, N. (2020). Cellulose-lignin composite fibres as precursors for carbon fibres. Part 2 - The impact of precursor properties on carbon fibres. *Carbohydrate Polymers*, 250, Article 116918. <https://doi.org/10.1016/j.carbpol.2020.116918>

This material is protected by copyright and other intellectual property rights, and duplication or sale of all or part of any of the repository collections is not permitted, except that material may be duplicated by you for your research use or educational purposes in electronic or print form. You must obtain permission for any other use. Electronic or print copies may not be offered, whether for sale or otherwise to anyone who is not an authorised user.

Journal Pre-proof

Cellulose-lignin composite fibres as precursors for carbon fibres. Part 2 -
The impact of precursor properties on carbon fibres

Nguyen-Duc Le (Conceptualization) (Investigation) (Formal analysis) (Writing - original draft) (Visualization), Mikaela Trogen (Resources) (Investigation) (Writing - review and editing), Yibo Ma (Investigation) (Writing - review and editing), Russell J. Varley (Supervision) (Writing - review and editing), Michael Hummel (Conceptualization) (Writing - review and editing) (Funding acquisition), Nolene Byrne (Conceptualization) (Supervision) (Writing - review and editing)



PII: S0144-8617(20)31091-2

DOI: <https://doi.org/10.1016/j.carbpol.2020.116918>

Reference: CARP 116918

To appear in: *Carbohydrate Polymers*

Received Date: 4 July 2020

Revised Date: 4 August 2020

Accepted Date: 4 August 2020

Please cite this article as: Le N-Duc, Trogen M, Ma Y, Varley RJ, Hummel M, Byrne N, Cellulose-lignin composite fibres as precursors for carbon fibres. Part 2 - The impact of precursor properties on carbon fibres, *Carbohydrate Polymers* (2020), doi: <https://doi.org/10.1016/j.carbpol.2020.116918>

This is a PDF file of an article that has undergone enhancements after acceptance, such as the addition of a cover page and metadata, and formatting for readability, but it is not yet the definitive version of record. This version will undergo additional copyediting, typesetting and review before it is published in its final form, but we are providing this version to give early visibility of the article. Please note that, during the production process, errors may be discovered which could affect the content, and all legal disclaimers that apply to the journal pertain.

© 2020 Published by Elsevier.

Cellulose-lignin composite fibres as precursors for carbon fibres. Part 2 - The impact of precursor properties on carbon fibres

Nguyen-Duc Le^a, Mikaela Trogen^b, Yibo Ma^b, Russell J. Varley^a, Michael Hummel^b and Nolene Byrne^{a,*}

a. Institute for Frontier Materials, Deakin University, Geelong, Vic 3217, Australia

b. Aalto University, School of Chemical Engineering, Department of Bioproducts and Biosystems, P.O. Box 16300, 00076 Aalto, Finland

* corresponding author: nolene.byrne@deakin.edu.au

Journal Pre-proof

Graphical abstract



Abstract: Carbon fibres, despite being responsible lightweight structures that improve sustainability through fuel efficiency and occupational safety, remain largely derived from fossil fuels. Alternative precursors such as cellulose and lignin (bio-derived and low cost) are rapidly gaining attention as replacements for polyacrylonitrile (PAN, an oil-based and costly precursor). This study uses a cellulose-lignin composite fibre, to elucidate the influence of precursor fabrication parameters (draw ratio and lignin content) on the efficiency of stabilisation and carbonisation, from the perspective of the chemical, morphological and mechanical changes. The degradation of cellulose chains was the primary contributor to the decrease in mechanical properties during stabilization, but is slowed by the incorporation of lignin. The skin-core phenomenon, a typical effect in PAN-based carbon fibres production, was also observed. Finally, the carbonization of incompletely stabilized fibres is shown to produce hollow carbon fibres, which have potential application in batteries or membranes.

Keywords: low-cost carbon fibers, cellulose-lignin composite fibers, skin-core fibers, hollow carbon fibers, cellulose lignin interaction.

1. Introduction:

Given their superior strength and light weighting potential, carbon fibres are a strategic material for aerospace, automotive manufacturing and military industries. Indeed the global demand for carbon fibres is expected to double every decade (Bohner, Weeber, Kuebler, & Steinhilper, 2015). Despite this, the application of carbon fibres remains limited to high-value products due to their relatively high costs, in part due to the fact that the raw material contributes about 53% of total production cost (Warren & Naskar, 2012). The development of low-cost alternative precursors therefore is imperative to reduce the overall cost. A wide variety of alternative precursors have been studied, but cellulose and lignin have gained the most attention due to their low-cost and wide availability from renewable resources.

Cellulose was used to produce the first carbon fibre in light bulbs by Thomas Edison in 1879 (Thomas Alva, 1879). Cellulose-based carbon fibres however, are limited because of their low carbon yield (10-30 % after carbonization) and because they require hot stretching to enhance mechanical strength (Huang, 2009). The subsequent introduction of polyacrylonitrile (PAN)-based carbon fibres with superior mechanical strength has since replaced cellulose-based carbon fibres, shrinking their market share drastically and remaining only as niche product for applications that require exceptionally high thermal resistance. Also lignin has experienced a renaissance as precursor material for carbon fibres Lignin is abundant biomass with millions of tons produced every year as by-product of the pulping industry. Lignin costs less than PAN with a significantly higher carbon yield than cellulose (62% vs 44% theoretically) (Frank, Steudle, Ingildeev, Spçrl, & Buchmeiser, 2014; Morgan, 2005). However, the current drawback for producing carbon fibres from lignin is the long stabilization times, which makes it impractical at the moment for industrial production (Bengtsson, Bengtsson, Sedin, & Sjöholm, 2019; Ogale, Zhang, & Jin, 2016).

In recent studies, composite fibres of lignin and cellulose have been prepared to overcome both disadvantages of cellulose and lignin (low carbon yield and long stabilization time, respectively) (Byrne et al., 2016; Ma et al., 2015). By using the ionic liquid (IL) 1,5-diazabicyclo[4.3.0]non-5-enium acetate ([DBNH]OAc), cellulose and lignin are co-dissolved to form a homogeneous solution. This so-called spin dope is used to make high-performance fibres by a dry-jet wet spinning method which can then be used in a continuous carbon production line (Ma et al., 2015). Olsson et al. 2017 and Bengtsson et al. 2019 reported successful conversion of cellulose-lignin composite fibres to carbon fibres on a lab scale with tensile strengths of 780 MPa and 1070 MPa, respectively (Bengtsson et al., 2019; Olsson, Sjöholm, & Reimann, 2017). Whilst these mechanical properties are still inferior to PAN-nased carbon fibres, they are nonetheless an extremely promising start for the development of a bio-derived carbon fibre.

This paper describes the effects of the structural characteristics of cellulose-lignin composite fibres on the stabilization and carbonization in an industrial-like carbonization line.

The preparation and mechanical properties of the precursor fibres and their thermal behaviour upon pyrolysis were discussed in detail in Part 1 of this study. Herein, different draws in the spinning process (ratio between extrusion speed and uptake speed) and lignin content of the precursor fibres were studied as described in **Table 1**. The evolution of the mechanical properties, chemical changes, graphitic structure and morphology of the resultant fibres during carbonisation was assessed and discussed.

Table 1: Precursor parameters

Sample ID	Lignin content (%)	Draw
30L DR3	30	3
30L DR6	30	6
30L DR12	30	12
50L DR3	50	3

2. Experimental:

2.1 Precursors:

Precursors were prepared by Aalto University from beech organosolv lignin powder and dissolving-grade pulp. Beech organosolv lignin was provided by the Fraunhofer Institutes, Center for Chemical-Biotechnological Processes (Germany) and was found to contain 96.4% lignin, 0.3% carbohydrates and 3.3% other material. Pre-hydrolysed kraft (PHK) birch pulp ($[\eta] = 494 \text{ ml/g}$; $M_w = 163.6 \text{ kg/mol}$) had a cellulose content of 91.7%, hemicellulose of 7.7%, and residual lignin content of 0.6% and was supplied by Stora Enso Enocell mill (Finland). More details on the raw materials and the composition of the spun fibers can be found in Part 1 of this study. The raw materials were dissolved in 1,5-diazabicyclo[4.3.0]non-5-enium acetate [DBNH]OAc with polymeric concentration 18wt.% to form a dope solution. The dope was heated to 70 °C before extruded from a 400-hole-spinneret. The extruded dope passed a 1 cm air gap before it was coagulated in a cold-water bath (15 °C), washed, dried and collected as continuous filament. The ratio between extrusion velocity and the uptake velocity defines the draw of the fibres.

2.2 Stabilization and carbonization:

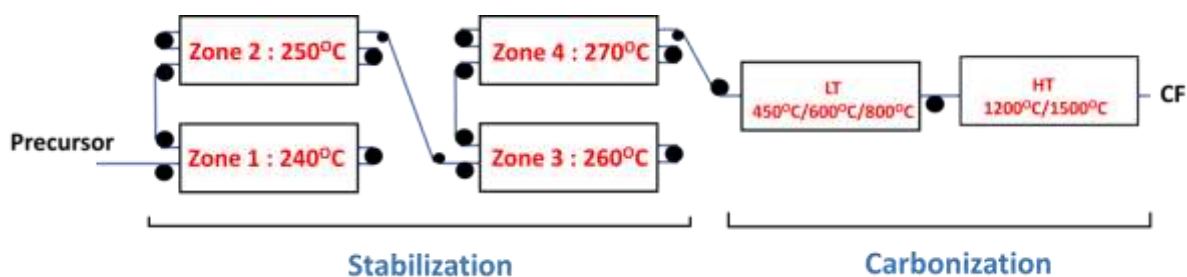


Figure 1: Process conditions during stabilization and carbonization

The carbon fibres production trial was conducted on the research line in Carbon Nexus, Deakin University, Australia. Precursors were oxidized through 4 zones before carbonized in a low temperature furnace and high temperature furnace. The detailed conditions were described in **Figure 1**. The tension was kept to a minimum because of the fragile nature of the fibres after stabilization. The line speed was also set low at 15.6 m/h to prevent fibre breakage. This resulted in a retention time of 23 min in each stabilization zone and 5.5 min in each carbonization furnaces, respectively.

2.3 Chemical and structural analysis:

2.3.1 Fourier Transformation Infrared spectroscopy (FTIR):

Chemical functional groups and their relative concentration were determined using FTIR spectroscopy conducted in the attenuated total reflection mode (ATR mode) using a Bruker Lumos. Each spectrum consisted of 32 scans from 650 to 4000 cm^{-1} at a resolution of 2 cm^{-1} .

2.3.2 Raman:

The graphitic structure of carbon fibres was studied using a Renishaw inVia system with 785 nm laser. Each sample was scanned 3 times and these data were accumulated to reduce the noise and enhance the signal-to-noise ratio. Peak fitting was processed on the accumulated data using Origin. A Lorentzian fitting function was used to fit the peak maxima.

2.3.3 Scanning electron microscope (SEM):

The morphology of the obtained samples was observed with a Zeiss Supra 55VP. Cross-section images were obtained through cryofracture. The fibre samples were immersed in liquid nitrogen until frozen. Then, they were taken out and snapped. Before measuring, all samples were sputter-coated with gold. 3.00 kV was used to prevent fibre damages.

2.3.4 Mechanical testing:

The single fibre testing was performed using Favimat+ (Textechno). The gauge length was 20 mm with 0.5 cN/tex pretension. For precursor testing, the test speed was 8 mm/min while for carbon fibre testing, the test speed was set lower at 2 mm/min due to the lower elongation to failure. A clamping force of 40 cN proved sufficient to avoid fibre slippage. Each sample was tested using 15 specimens to obtain the result.

3. Results and discussions

3.1 Mechanical properties as a function of draw and lignin content:

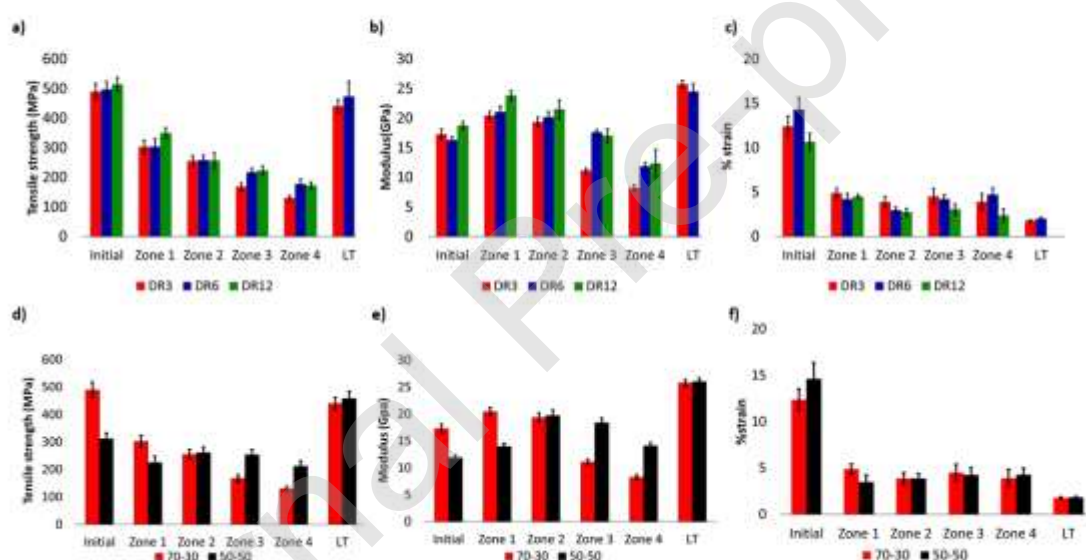


Figure 2: Mechanical properties of 30% lignin fibres at different draw ratios: a) Tensile strength, b) Modulus, c) % strain; and fibres spun at DR3 with various lignin content: d) Tensile strength, e) Modulus, f) % strain

The precursor fibres were stabilized by passing through 4 oxidative zones and carbonized in a low temperature furnace and high temperature furnace. **Figure 2a** and **Figure 2d** show the tensile strength of samples as a function of draw and lignin content taken from the 4 oxidative zones and the LT furnace of the carbonisation line. Samples from the HT furnace were not able to be measured due to extensive fusion of the fibres after carbonisation. As can be seen, as the precursors are heated and undergo stabilization, the tensile strength decreases with the lowest tensile strength occurring

in zone 4. The tensile strength of the composite fibres behaves similarly to cellulose fibres during a similar temperature range reported elsewhere (Bacon, 1973; Plaisantin et al., 2006), while the tensile strength of the lignin fibres remains stable and intact at this stage (Kleinhans & Salmén, 2016). This indicates that the influence of cellulose degradation upon the properties of the composite fibres during stabilization decreases when the lignin content increases (**Figure 2d**). Once carbonization commences, the tensile strength increases as the graphitic structure of carbon fibre begins to form. (Bacon, 1973; Kleinhans & Salmén, 2016). Moreover, the tensile strengths after LT treatment for the 30L and 50L samples indicate no significant difference, suggesting the dominant role of the newly formed graphitic structure in controlling properties.

Figure 2b shows the modulus of 30L samples as a function of draw for samples taken from the various oxidative zones and the LT furnace, while **Figure 2e** shows the modulus as a function of lignin content. Unlike the tensile strength, the modulus increases in the first stabilization zone but subsequently decreases until oxidation zone 4. Again, as per the strength, once carbonisation is initiated in the LT furnace, the modulus increases dramatically. This trend is similar to what has been found for carbonisation studies of cellulose fibres (Bacon, 1973; Plaisantin et al., 2006), which also produced an initial increase followed by a decreased with extended stabilisation. In comparison, the modulus of the lignin fibres decreased slightly during the stabilization (Kleinhans & Salmén, 2016). **Figure 2c and Figure 2f** illustrate the decreasing strain of the fibres as they transition from precursors (10-12%) to stabilized products (3-5%) and finally to carbonized products (2%). This clearly demonstrates the transition from a ductile thermoplastic polymer to one that is brittle and crosslinked. This transformation also happens to cellulose precursor during the stabilization (Bacon, 1973), although Kleinhans et al. found that the strain to failure of the lignin fibres increased during this time (Kleinhans & Salmén, 2016) which was attributed to the reduction of crosslinking in lignin that increases the flexibility of the fibres.

Figure 2 a, b and c suggest that there is no significant difference between the samples produced with different draw ratios, with all showing a decreasing trend in the mechanical properties during stabilization. This is likely due to the similarity of the crystallinity and orientation of polymer chains in the precursor fibres. The difference in the degree of crystallinity and orientation of the cellulose crystals between the precursor fibres was not significant (Ma et al., 2015). Therefore, despite differences in fibre diameter, no significant difference in mechanical properties was evident. Meanwhile, **Figure 2 d, e, and f** suggest a minor influence of the lignin content on the mechanical properties of during the stabilization. Tensile strength and modulus after zones 3 and 4 are slightly higher in the case of 50L. However, the differences disappear instantly after carbonization in the LT furnace.

3.2 Chemical change as a function of zones and lignin content:

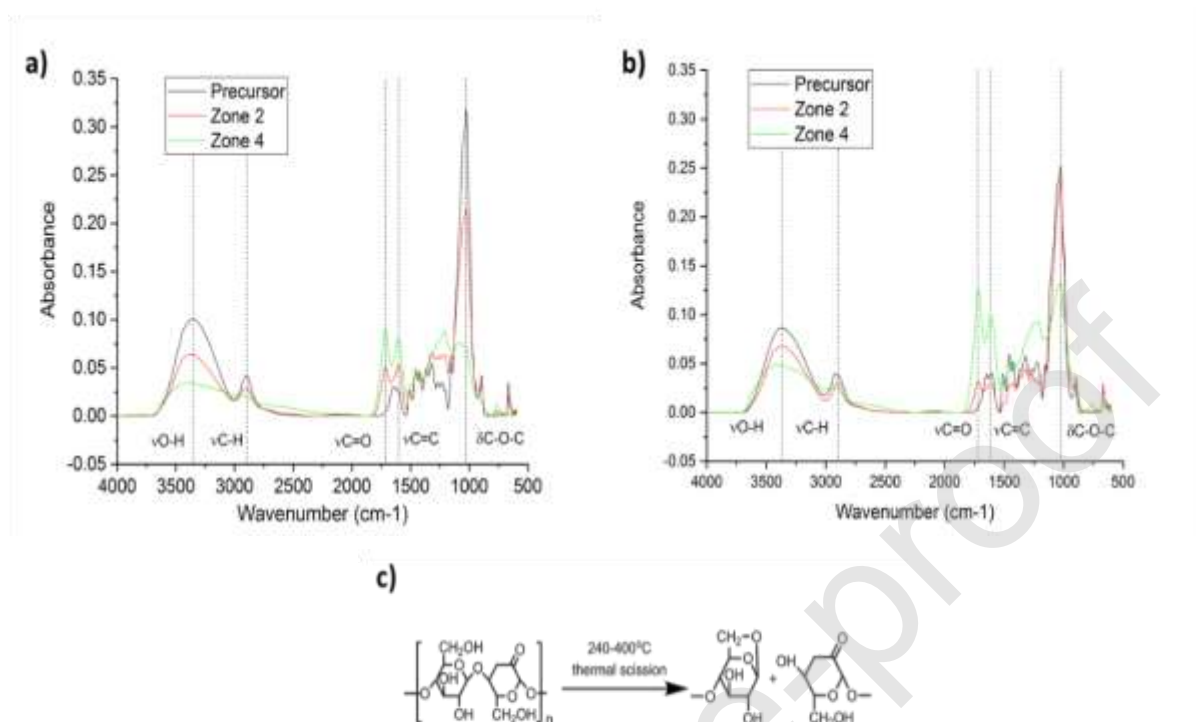


Figure 3: FTIR spectrum of a) 70-30 b) 50-50 and c) illustration of cellulose thermal scission.

Table 2: Peak intensity change as a function of zones

Peak	50-50			70-30		
	Zone 2	Zone 4	% change of zone 4 vs zone 2	Zone 2	Zone 4	% change zone 4 vs zone 2
O-H	2.126	0.710	33.40	2.094	0.087	4.15
C-O-C	7.701	3.603	46.79	7.530	1.275	16.93
C=O	0.980	2.833	289.20	0.886	2.129	240.18
C=C	0.943	2.136	226.53	0.873	1.922	220.12

Figure 3a and **b** show the IR spectra of precursor and oxidized products for 30L and 50L. Since the 30L and 50L samples both contain cellulose and lignin, it is not surprising they exhibit similar chemical changes in the IR during carbonisation. Both cellulose and lignin exhibit decreasing -OH (3300 cm^{-1}) and C-O-C groups (1024 cm^{-1}),

due to degradative chain scission, and increasing C=O groups (1718 cm^{-1}) from oxidation and increasing C=C (1606 cm^{-1}) arising from the dehydration of the polymer backbone. The loss of -OH groups during pyrolysis compromises the structure of the cellulose crystals (Tang & Bacon, 1964), which are connected through weak hydrogen bonding (bonding energy from 8.5 to 15 kJ/mol) (Mudgil, 2017; Zhibankov & Kozlov, 1983). When heat is applied during stabilization, these linkages between the polymer chains are disrupted easily which destroys the cellulose crystals and leads to a sudden drop in the strain value when the cellulose is stabilised (Tang & Bacon, 1964).

The gradual decrease in tensile strength and modulus arises from the conversion of cellulose chains. As proposed by Tang and Bacon (**Figure 3c**), the pyrolysis mechanism involves the breakage of the cellulose backbone (C-O-C bonds), depolymerizing cellulose chains and reducing strength and Young's modulus during stabilization (Tang & Bacon, 1964).

Despite both 30L and 50L have the same pyrolysis reactions for cellulose and lignin, the difference in chemical composition leads to a difference in the reaction rate. In order to better understand these differences, the change in peak intensity was calculated by using C-H peak (1440 cm^{-1}) as an internal standard (Byrne, De Silva, Ma, Sixta, & Hummel, 2018). The results in **Table 2** show that the increase in peak intensity of the C=C bonds and C=O bonds, (oxidation and olefin formation) is significantly higher for the 50L compared with the 30L. In contrast, the reduction of O-H and C-O-C groups from cellulose for the 50L is less than for the 30L sample, especially in zone 4. This suggests that a higher lignin content is able alter the pyrolysis reactions of cellulose. Lignin seems to promote the dehydration reaction and prevent the thermal cleavage of glycosidic bonds (C-O-C bond), respectively (Zhang et al., 2015). As a result, the decrease of mechanical properties in 50L is slower than 30L.

3.3 Carbon structure change as a function of carbonized temperature:

The carbon structure of fibres with various draw and lignin content were studied by Raman spectroscopy on carbon fibres. The obtained results for the low temperature and the high-temperature furnace are shown in **Figure 4**. Typical Raman peaks for carbon are D (1360 cm^{-1}), A (1480 cm^{-1}), G (1584 cm^{-1}) and D' (1680 cm^{-1}) (Jawhari, Roid, & Casado, 1995; D. Li et al., 2014; Melanitis, Tetlow, & Galiotis, 1996; Xue, Liu, Lian, & Liang, 2013). The G-band accounts for the sp^2 bonding of the C=C bonds in the graphitic structure; whereas the D band represents sp^3 bonding which is related to disorder in the graphitic structure. Therefore, the ratio of the D band over the G band (I_D/I_G) represents for the order level in graphitic structure (Gruen et al., 1998; Kowalewski, Tsarevsky, & Matyjaszewski, 2002; Yan & Barron, 2017). Amorphous carbonaceous structures are accounted by A-band (Xue et al., 2013). The D' band visible as shoulder of the G band also represents the disorder of the graphitic

structure. Peak deconvolution using Lorentzian fitting functions was performed to isolate the individual contributions (Nunna et al., 2016) (**Figure 4**). The calculated results are shown in **Table 3**.

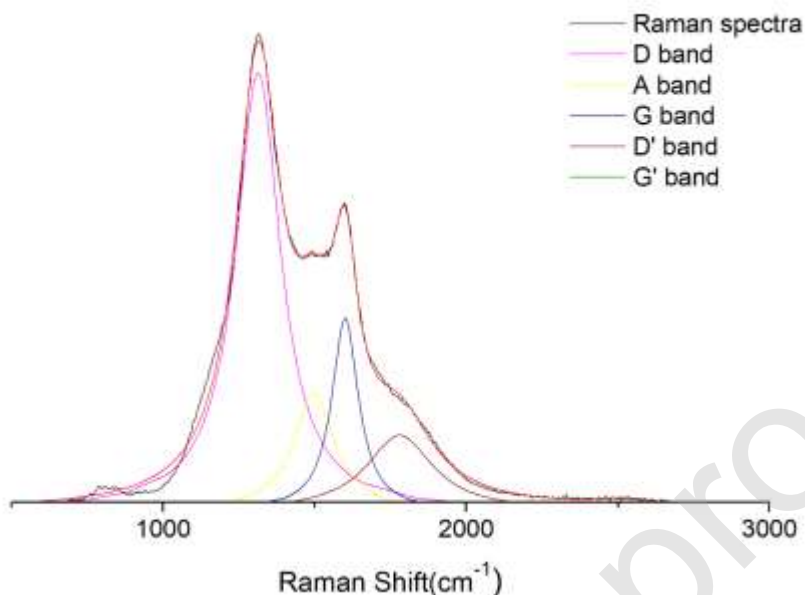


Figure 4: Lorentz curve fit on the Raman spectra

Table 3: Calculated data from Raman spectrum

Samples	LT				HT			
	FWHM _D	FWHM _G	I _D /I _G	Crystal size nm	FWHM _D	FWHM _G	I _D /I _G	Crystal size nm
50-50 DR3	242.87	139.78	1.28	18.56	191.71	170.61	1.56	15.22
70-30 DR3	240.48	135.67	1.26	18.76	202.62	156.92	1.52	15.56
70-30 DR6	240.22	134.13	1.27	18.64	197.15	133.85	1.55	15.30
70-30 DR12	244.93	132.85	1.28	18.52	194.97	142.42	1.58	15.01

The Tuinstra–Koenig equation allows for the calculation of the crystal size of the graphitic clusters:

$$L_a(\text{nm}) = \frac{4.4}{\frac{I_D}{I_G}}$$

The original Tuinstra–Koenig equation is valid for a 515 nm laser source. However, this measurement was conducted with 785nm laser source. Thus, the energy

dependence was taken into account to correct for the different laser source (Mallet-ladeira et al., 2014) :

$$L_a(nm) = \frac{4.4}{\frac{I_D}{I_G}} \times \left(\frac{2.41}{E_L(eV)} \right)^4$$

where for 785 nm, the energy $E_{785\text{ nm}} = \frac{h.c}{\text{wave length}} = \frac{1240\text{ eV nm}}{784\text{ nm}} = 1.582\text{ eV}$

$$L_{785}(nm) = \frac{4.4}{\frac{I_D}{I_G}} \times \left(\frac{2.41}{1.582} \right)^4 = \frac{I_G}{I_D} \times 23.70\text{ nm}$$

This corrected equation was used to calculate the graphitic crystal size for the samples investigated herein (**Table 3**). The Raman spectra are plotted in **Figure 4**, which clearly shows the existence of the D, G, and D' bands. The A band (the amorphous carbon) is covered by the D and G bands and is only apparent after deconvolution of the peaks. As mentioned above, the high value of the I_D/I_G and the existence of D' band and A band suggest that the graphitic structure of carbon fibres has many defects, is strongly amorphous and has low levels of crystallinity. Moreover, the I_D/I_G value indicates a turbostratic carbon structure in the CFs (Ogale et al., 2016). From the calculated data shown in **Table 3**, the crystallite sizes are similar between the different draw ratios with the crystal sizes (L_a) after of treatment in the HT furnace being smaller than after treatment in the LT furnace. It is proposed that high temperatures cause a refinement effect which modifies the graphite crystallites by removing carbon atoms and reducing the crystallite size (Sazali et al., 2016).

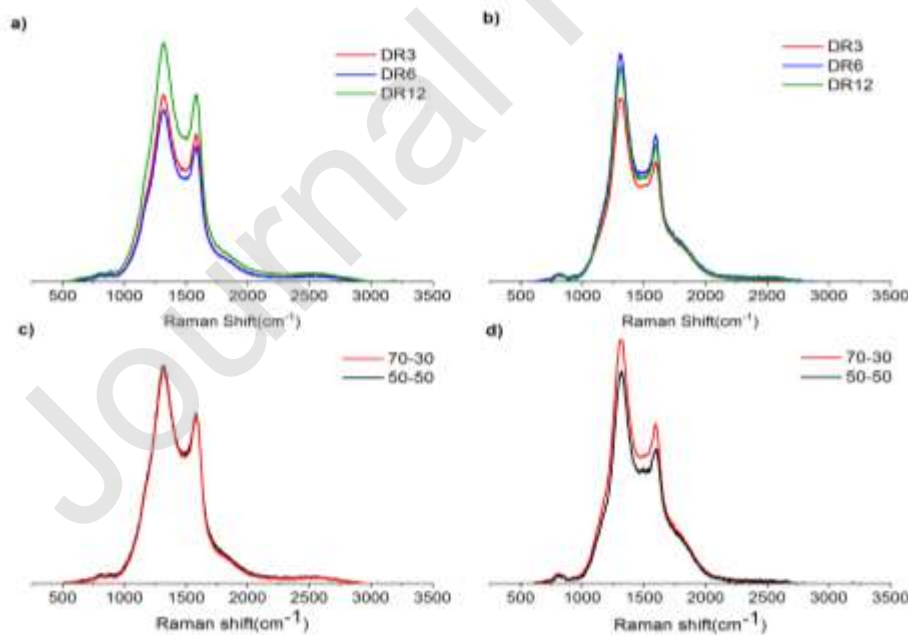


Figure 5: Raman spectra of fibres spun at different draw: a) low temperature furnace b) high temperature furnace; and spectra of fibres with different lignin content c) low temperature furnace d) high temperature furnace

No difference in the Raman spectra was observed as a function of draw. Therefore, it can be stated that there is little to no influence on the graphitic structure caused by the draw. For 30L fibres, cellulose accounts for 70 wt%, so most of the graphitic structure is originated from the cellulose crystals in the blend fibres. The difference in crystallinity for 30L fibres spun at different draw is relatively small (see Part 1 of this study) and explain the similarity in graphitic structure of the resulting carbon fibres. Eventually, this is reflected in their similar mechanical properties.

The comparison between the Raman spectra of 50L and 30L fibres is shown in **Figure 5c** and **5d**. Since lignin has greater aromaticity in the backbone, increasing the lignin share would be expected to increase the graphite layers in CFs structure (phenyl-plane structure (Saito & Arima, 2002; Wang, Okazaki, Suzuki, & Funaoka, 2003) or highly-condensed aromatic structure (Cao, Xiao, Xu, Shen, & Jin, 2013)). However, from the calculated data in **Table 3**, the I_D/I_G ratio is similar between 50L and 30L samples, suggesting a similar graphitic structure which is complemented by the observed similarity in mechanical properties. This finding means that addition of lignin does not increase the graphitic structure in carbon fibres and supports the idea that lignin is a non-graphitizable material (hard carbon) (Dallmeyer, Lin, Li, Ko, & Kadla, 2014; Y. Li, Cui, Tong, & Xu, 2013; Poursorkhabi, Mohanty, & Misra, 2016).

3.4 Morphology changes as a function of draw and carbon content:

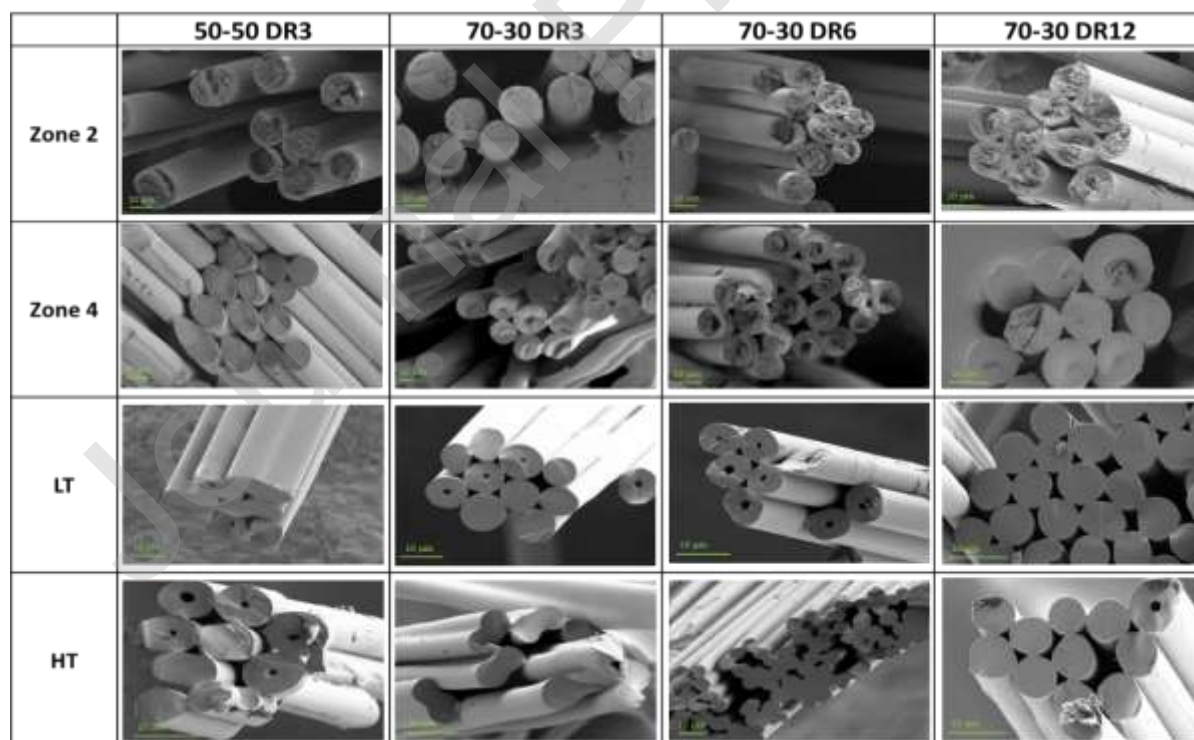


Figure 6: SEM images of stabilized and carbonized products from different precursor fibres and obtained after different zones as indicated in the illustration.

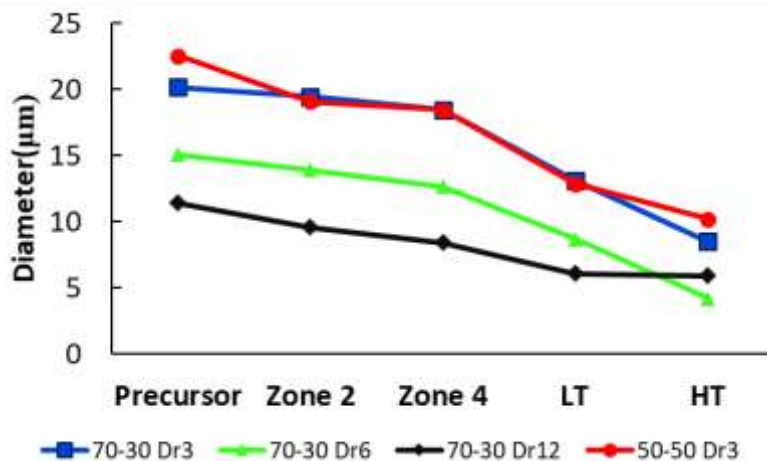


Figure 7: Diameter of the single filament after each zone.

The morphology changes of the composite fibres after passing through all zones are shown in **Figure 6**. Treatment in zone 2 produces a skin-core phenomenon whereby the skin is stabilized but the core appears to be largely the same as the precursor structure. In addition, there appears to be internal connections between filaments caused by the deposition of volatile compounds at the contact points (Ford & Mitchell, 1963). At zone 4, the skin-core phenomenon has virtually disappeared due to further thermal and oxidative treatment, but the precursor structure can still be observed in some filaments. Furthermore, the fusion of fibres is also more prevalent. After the low temperature (LT) furnace, the precursor structure has disappeared, and the fibre surface becomes smoother, indicative of a high carbon content after carbonization. The formation of partly hollow fibre may be attributed to the skin-core formation of stabilized fibres. The unstabilized core of stabilized fibres decomposed and created voids inside fibre (hollow structure). This phenomenon is subject of future investigations. High temperature (HT) furnace samples have no significant change in comparison with low temperature furnace samples but showed fusion of individual filaments. The deposition and re-condensation of volatile carbonaceous compounds can be avoided by adjusting the retention time and gas flow in the HT furnace. This is a shortcoming of the employed carbonization line, which was primarily designed for PAN-fibres. The retention times in the different zones are connected. Further optimization studies, preferably offline, are also required here.

The fibre diameter slowly reduces during stabilization but reduced markedly during carbonization, along with a large mass loss. This finding was confirmed with TGA results of composite fibres (Ma et al., 2015), where most weight loss happens after 350°C (see also Part 1). The fibre diameter also depends on draw, with higher draw leading to smaller fibre diameter. In contrast, the fibre diameters of 50L and 30L are similar, despite differences in chemical composition.

4. Conclusion:

This study investigated the impact of different draw and lignin content on the chemical changes and mechanical properties of the stabilised precursor and carbon fibre made from cellulose-lignin composite fibres. The results revealed the importance of controlling the balance between pyrolysis and carbonization reactions to achieve excellent mechanical properties during stabilization and carbonization. It was shown that the pyrolysis of cellulose polymer chains reduced the mechanical properties during stabilization, but could be mitigated by the more thermally stable lignin. In contrast, different draw ratios in the production of the precursor fibers had no impact on the mechanical properties of fibres during stabilization. Another noticeable finding is how lignin carbonizes and forms the carbon structure. Lignin is a non-graphitizable compound, so the carbon fibres from lignin cannot achieve high mechanical strength without any treatment to improve the graphitic structure (Sagues et al., 2019) The skin-core phenomenon, however, was observed in Zone 2 but disappeared in Zone 4 and was attributed to the incomplete stabilization of precursor fibres. It was found that this led to the formation of hollow carbon fibres after carbonization which have very high surface areas, providing promise for applications in batteries, catalyst carriers or membranes (Liu, Chae, Choi, & Kumar, 2015).

Author contributions (CRediT)

Nguyen-Duc Le: Conceptualization, Investigation, Formal analysis, Writing - Original Draft, Visualization.

Mikaela Trogen: Resources, Investigation, Writing - Review & Editing.

Yibo Ma: Investigation, Writing - Review & Editing.

Russell J. Varley: Supervision, Writing - Review & Editing.

Michael Hummel: Conceptualization, Writing - Review & Editing, Funding acquisition.

Nolene Byrne: Conceptualization, Supervision, Writing - Review & Editing.

5. Acknowledgements:

MT and MH have received funding from the European Research Council (ERC) under the European Union's Horizon 2020 research and innovation programme (grant agreement No 715788).

6. References:

- Bacon, R. (1973). Carbon fibers from rayon precursors. *Chemistry and Physics of Carbon*, 9.
- Bengtsson, A., Bengtsson, J., Sedin, M., & Sjöholm, E. (2019). Carbon Fibers from Lignin-Cellulose Precursors: Effect of Stabilization Conditions. *ACS Sustainable Chemistry & Engineering*, 7(9), 8440–8448.
- Bohner, J., Weeber, M., Kuebler, F., & Steinhilper, R. (2015). Developing a learning factory to increase resource efficiency in composite manufacturing processes BT - 5th Conference on Learning Factories 2015, July 7, 2015 - July 8, 2015. In *Elsevier* (Vol. 32, pp. 64–69). <https://doi.org/10.1016/j.procir.2015.05.003>
- Byrne, N., De Silva, R., Ma, Y., Sixta, H., & Hummel, M. (2018). Enhanced stabilization of cellulose-lignin hybrid filaments for carbon fiber production. *Cellulose*, 25(1), 723–733. <https://doi.org/10.1007/s10570-017-1579-0>
- Byrne, N., Setty, M., Blight, S., Tadros, R., Ma, Y., Sixta, H., & Hummel, M. (2016). Cellulose-Derived Carbon Fibers Produced via a Continuous Carbonization Process: Investigating Precursor Choice and Carbonization Conditions. *Macromolecular Chemistry and Physics*, 217(22), 2517–2524. <https://doi.org/10.1002/macp.201600236>
- Cao, J., Xiao, G., Xu, X., Shen, D., & Jin, B. (2013). Study on carbonization of lignin by TG-FTIR and high-temperature carbonization reactor. *Fuel Processing Technology*, 106, 41–47. <https://doi.org/10.1016/j.fuproc.2012.06.016>
- Dallmeyer, I., Lin, L. T., Li, Y., Ko, F., & Kadla, J. F. (2014). Preparation and Characterization of Interconnected, Kraft Lignin-Based Carbon Fibrous Materials by Electrospinning. *Macromolecular Materials and Engineering*, 299(5), 540–551. <https://doi.org/10.1002/mame.201300148>
- Ford, C. E., & Mitchell, C. V. (1963). Fibrous graphite. *US Patent 3,107,152*, 1–5. Retrieved from <https://patents.google.com/patent/US3107152A/en>
- Frank, E., Stuedle, L. M., Ingildeev, D., Spçrl, J. M., & Buchmeiser, M. R. (2014). Carbon Fibers: Precursor Systems, Processing, Structure, and Properties. *Angew. Chem. Int. Ed*, 53, 5262–5298. <https://doi.org/10.1002/anie.201306129>
- Gruen, D. M., Krauss, A. R., Zuiker, C. D., Csencsits, R., Terminello, L. J., Carlisle, J. A., ... Himpfel, F. J. (1998). Characterization of nanocrystalline diamond films by core-level photoabsorption. *Applied Physics Letters*, 68(12), 1640. <https://doi.org/10.1063/1.115677>
- Huang, X. (2009). Fabrication and Properties of Carbon Fibers. *Materials*, 2(4), 2369–2403. <https://doi.org/10.3390/ma2042369>
- Jawhari, T., Roid, A., & Casado, J. (1995). Raman spectroscopic characterization of some commercially available carbon black materials. *Carbon*, 33(11), 1561–1565. [https://doi.org/10.1016/0008-6223\(95\)00117-V](https://doi.org/10.1016/0008-6223(95)00117-V)
- Kleinhans, H., & Salmén, L. (2016). Development of lignin carbon fibers: Evaluation of the carbonization process. *Journal of Applied Polymer Science*, 133(38). <https://doi.org/10.1002/app.43965>
- Kowalewski, T., Tsarevsky, N. V., & Matyjaszewski, K. (2002). Nanostructured carbon arrays from block copolymers of polyacrylonitrile. *Journal of the American Chemical Society*, 124(36),

10632–10633. <https://doi.org/10.1021/ja0178970>

- Li, D., Lu, C., Wu, G., Yang, Y., An, F., Feng, Z., & Li, X. (2014). Structural heterogeneity and its influence on the tensile fracture of PAN-based carbon fibers. *RSC Adv.*, *4*(105), 60648–60651. <https://doi.org/10.1039/C4RA08530B>
- Li, Y., Cui, D., Tong, Y., & Xu, L. (2013). Study on structure and thermal stability properties of lignin during thermostabilization and carbonization. *International Journal of Biological Macromolecules*, *62*, 663–669. <https://doi.org/10.1016/J.IJBIOMAC.2013.09.040>
- Liu, Y., Chae, H. G., Choi, Y. H., & Kumar, S. (2015). Preparation of low density hollow carbon fibers by bi-component gel-spinning method. *Journal of Materials Science*, *50*(10), 3614–3621. <https://doi.org/10.1007/s10853-015-8922-3>
- Ma, Y., Asaadi, S., Johansson, L.-S., Ahvenainen, P., Reza, M., Alekhina, M., ... Sixta, H. (2015). High-Strength Composite Fibers from Cellulose-Lignin Blends Regenerated from Ionic Liquid Solution. *ChemSusChem*, *8*(23), 4030–4039. <https://doi.org/10.1002/cssc.201501094>
- Mallet-ladeira, P., Puech, P., Toulouse, C., Cazayous, M., Ratel-ramond, N., Weisbecker, P., ... Monthieux, M. (2014). A Raman study to obtain crystallite size of carbon materials : A better alternative to the Tuinstra – Koenig law. *Carbon*, *80*, 629–639. <https://doi.org/10.1016/j.carbon.2014.09.006>
- Melanitis, N., Tetlow, P. L., & Galiotis, C. (1996). Characterization of PAN-based carbon fibres with laser Raman spectroscopy. *Journal of Materials Science*, *31*(4), 851–860. <https://doi.org/10.1007/BF00352882>
- Morgan, P. (2005). *Carbon fibers and their composites. Carbon Fibers and Their Composites.* <https://doi.org/10.1016/j.tube.2011.07.006>
- Mudgil, D. (2017). The Interaction Between Insoluble and Soluble Fiber. *Dietary Fiber for the Prevention of Cardiovascular Disease*, 35–59. <https://doi.org/10.1016/B978-0-12-805130-6.00003-3>
- Nunna, S., Naebe, M., Hameed, N., Creighton, C., Naghashian, S., Jennings, M. J., ... Fox, B. L. (2016). Investigation of progress of reactions and evolution of radial heterogeneity in the initial stage of thermal stabilization of PAN precursor fibres. *Polymer Degradation and Stability*, *125*, 105–114. <https://doi.org/10.1016/J.POLYMDEGRADSTAB.2016.01.008>
- Ogale, A. A., Zhang, M., & Jin, J. (2016). Recent advances in carbon fibers derived from biobased precursors. *Journal of Applied Polymer Science*, *133*(45). <https://doi.org/10.1002/app.43794>
- Olsson, C., Sjöholm, E., & Reimann, A. (2017). Carbon fibres from precursors produced by dry-jet wet-spinning of kraft lignin blended with kraft pulps. *Holzforschung*, *71*(4), 275–283. <https://doi.org/10.1515/hf-2016-0189>
- Plaisantin, H., Pailler, R., Guette, A., Birot, M., Pillot, J.-P., Daude, G., & Olry, P. (2006). Ex-cellulose carbon fibres with improved mechanical properties. *Journal of Materials Science - J MATER SCI*, *41*, 1959–1964.
- Poursorkhabi, V., Mohanty, A. K., & Misra, M. (2016). Statistical analysis of the effects of carbonization parameters on the structure of carbonized electrospun organosolv lignin fibers. *Journal of Applied Polymer Science*, *133*(45). <https://doi.org/10.1002/app.44005>
- Sagues, W., Jain, A., Brown, D., Aggarwal, S., Suarez, A., Kollman, M., ... Argyropoulos, D. (2019). Are

- Lignin-Derived Carbon Fibers Graphitic Enough? *Green Chemistry*, 21. <https://doi.org/10.1039/C9GC01806A>
- Saito, Y., & Arima, T. (2002). Growth of cone-shaped carbon material inside the cell lumen by heat treatment of wood charcoal. *Journal of Wood Science*, 48(5), 451–454. <https://doi.org/10.1007/BF00770709>
- Sazali, N. E. S., Deraman, M., Omar, R., Othman, M. A. R., Suleman, M., Shamsudin, S. A., ... Basri, N. H. (2016). Preparation and structural characterization of turbostratic-carbon/graphene derived from amylose film. In *AIP Conference Proceedings* (Vol. 1784, p. 040009). AIP Publishing LLC. <https://doi.org/10.1063/1.4966795>
- Tang, M., & Bacon, R. (1964). Carbonization of cellulose fibers—I. Low temperature pyrolysis. *Carbon*, 2(3), 211–220. [https://doi.org/10.1016/0008-6223\(64\)90035-1](https://doi.org/10.1016/0008-6223(64)90035-1)
- Thomas Alva, E. (1879). Electric lamp. *UNITED STATES PATENT US223898TA*. <https://doi.org/10.1136/bmj.1.1157.435-b>
- Wang, X.-S., Okazaki, N., Suzuki, T., & Funaoka, M. (2003). Effect of Calcium on the Catalysis of Nickel in the Production of Crystallized Carbon from Lignocresol for Electromagnetic Shielding. *Chemistry Letters*, 32(1), 42–43. <https://doi.org/10.1246/cl.2003.42>
- Warren, C. D., & Naskar, A. K. (2012). Lower cost carbon fiber precursors. In *Presentation at 2012 DOE Hydrogen and Fuel Cells Program and Vehicle Technologies Program Annual Merit Review and Peer Evaluation Meeting, Arlington, VA, USA* (Vol. 16).
- Xue, Y., Liu, J., Lian, F., & Liang, J. (2013). Effect of the oxygen-induced modification of polyacrylonitrile fibers during thermal-oxidative stabilization on the radial microcrystalline structure of the resulting carbon fibers. *Polymer Degradation and Stability*, 98(11), 2259–2267. <https://doi.org/10.1016/J.POLYMDEGRADSTAB.2013.08.016>
- Yan, Z., & Barron, Andrew R. (2017). *Characterization of Graphene by Raman Spectroscopy Raman spectrum of graphene The G - band*. Retrieved from <https://cnx.org/contents/8GImxcKk@2/Characterization-of-Graphene-b>
- Zhang, J., Choi, Y. S., Yoo, C. G., Kim, T. H., Brown, R. C., & Shanks, B. H. (2015). Cellulose–Hemicellulose and Cellulose–Lignin Interactions during Fast Pyrolysis. *ACS Sustainable Chemistry & Engineering*, 3(2), 293–301. <https://doi.org/10.1021/sc500664h>
- Zhbankov, R. G., & Kozlov, P. V. (1983). Fizika tsellyulozy i ee proizvodnykh. *The Physics of Cellulose and Its Derivatives*, Izd. Nauka i Tekhnika, Minsk.